PROCEEDINGS, 41st Workshop on Geothermal Reservoir Engineering
Stanford University, Stanford, California, February 22-24, 2016
SGP-TR-209

Application of numerical methods for geothermal pressure transient analysis: A deflagration case study from New Zealand

Katie McLean[1]*, Sadiq J. Zarrouk[1], Daniel Wilson[2]

[1] Department of Engineering Science, University of Auckland, Private Bag 92019, Auckland, New Zealand

[2] Contact Energy Ltd, Wairakei Power Station, Taupo, New Zealand

*pmcl037@aucklanduni.co.nz

Keywords: Pressure transient analysis, well testing, geothermal, numerical modelling, TOUGH2, PyTOUGH, deflagration, derivative plot.

ABSTRACT

Numerical models to simulate geothermal pressure transients are required in place of analytical models. This is due to the high temperature and complexity of geothermal reservoirs as compared to oil and gas reservoirs for which analytical models were developed. No numerical tool for this application is currently available to the geothermal industry. However the recent development of PyTOUGH for automating TOUGH2 simulations has enabled the use of TOUGH2 for geothermal well test analysis with relative ease. A standard model design has recently been developed using PyTOUGH, specifically for pressure transient analysis. PyTOUGH is used to automate the creation of the model grid and input file, running the model, extraction of results and comparison with field data.

In this study the numerical PyTOUGH/TOUGH2 standard model setup is demonstrated through a case study using field data from the Ohaaki geothermal field, New Zealand. Investigation is made into the choice of method to evaluate model layer thickness and model injectate temperature, and the impact of these choices on the results. Field data used are pressure fall-off transients from injection tests performed immediately before and after deflagration of a well. The results of pressure transient analysis are examined to determine the effect of deflagration on permeability in the skin zone and wider reservoir. These results and the overall change in injectivity index are used to draw conclusions on the efficacy of the deflagration. The contribution of thermal permeability enhancement is also considered. The results from numerical models are compared with the results obtained by applying conventional analytical models.

1. INTRODUCTION

The application of analytical models to geothermal pressure transient analysis (PTA) is problematic as many of the necessary simplifying assumptions are violated in the geothermal environment. This is primarily the result of high temperature and large reservoir thickness and complexity. One key issue for geothermal injection testing is the large differential in temperature and therefore fluid properties between cold injectate and hot reservoir, which cannot be accounted for by analytical models.

Recent developments have enabled the use of the numerical simulator TOUGH2 for the analysis of geothermal pressure transients. A standard model design has been developed, the use of which will promote comparability of results across the geothermal industry. The standard model setup utilises TOUGH2 and is automated using the PyTOUGH scripting library, which greatly enhances the capability and user-friendliness of the model. The reservoir type currently implemented in the numerical model is a uniform porous reservoir. Boundary types include an infinite reservoir with no boundary, a single linear impermeable boundary and a channel bounded by two linear impermeable boundaries. The standard model design includes wellbore storage and the skin factor.

In this work, the new numerical tools are demonstrated on two datasets from Ohaaki geothermal field, New Zealand. The two datasets are pressure fall-off transients from injection testing carried out immediately before and after deflagration. The results of the numerical modelling will be compared to the results obtained from analytical modelling utilising the software SAPHIR™. Particular focus will be on the reservoir permeability, skin factor and the shape of the pressure derivative plot.

2. BACKGROUND

2.1 Numerical modelling of geothermal pressure transients

The need for numerical models to simulate geothermal pressure transients has been long recognised. This is due to the fundamental differences between geothermal and oil and gas reservoirs, and the simplifying assumptions of the analytical models which do not hold in the geothermal environment. A standard model setup has recently been proposed for this purpose (McLean and Zarrouk, 2015a). This utilises the AUTOUGH2 version (Yeh, Croucher and O'Sullivan, 2012) of the TOUGH2 simulator (Pruess, 1991). Automation of the simulation setup, running and extraction of results is enabled by PyTOUGH (Croucher, 2011). The standard setup as described is effectively an equivalent to the uniform porous infinite reservoir model, familiar from analytical model analysis.

The standard reservoir model setup takes account of the injectate temperature as well as the reservoir temperature. It has been concluded that injection of cold water into a hot reservoir produces a pressure derivative response with a large hump in early and intermediate-time very similar to positive skin (McLean and Zarrouk, 2015b). An equivalent to the linear impermeable boundary model has been created by using PyTOUGH to modify the block volumes and surface areas within the model as if there is a linear impermeable boundary near the well (McLean and Zarrouk, 2015c). This produces a pressure derivative response very similar in shape to the analytical model equivalent.

The standard model setup produces results which have been shown to be sensitive to the layer thickness used (McLean and Zarrouk, 2015a). The same model thickness must be used in order to compare results.

2.2 General deflagration process

The deflagration process is a well stimulation method which delivers a high pressure impulse down hole. The pressure impulse is generated by igniting a solid propellant charge (solid rocket fuel) to rapidly create a gas cloud which is intended to open up and enhance existing fractures. The deflagration tool is conveyed by an E-line and consists of a perforated hollow steel carrier to house the propellant, a detonator and a casing collar locator (CCL) sitting on top of the carrier. The setup is similar to a wireline-deployed perforating gun. Due to the nature of geothermal wells and the high temperature instability of the propellant and detonator the well needs to be quenched to below 204°C.

For a successful deflagration job it is important to have an accurate target zone identified, either during the pre-job injectivity test or from earlier completion testing and borehole imaging. At least 400m of water is required above the tool to provide pressure support and also act as a shock absorber and accelerator much like in a drilling jar assembly. The deflagration gun is lowered to the target zone and detonated from the surface via the wireline firing panel. The actual event time is between 300-600 milliseconds depending on the setup parameters. Deflagration is a near-wellbore permeability enhancement tool and the penetration is dependent on fracture plane volume and orientation. The deflagration technique is used predominantly in the oil and gas industry as a pre-hydrofrac treatment and also a multi-zone treatment without the need to isolate individual zones. Deflagration can also be used as a scale treatment to knock off scale from production strings.

2.3 Geothermal deflagration studies

The use of deflagration in geothermal wells is limited for a variety of reasons. Only recently has a deflagration tool become available that is capable of withstanding temperatures of up to 204°C without detonating prematurely. Also, geothermal wells have extensive open-hole sections as compared to narrow perforated zones in oil and gas wells and so the identification of the permeable feed zones within the open-hole is critical. However geothermal wells typically have many feed zones and their identification is fundamentally complex and subjective. There are however a few published studies of geothermal deflagration at Soda Lake, USA, Reykjanes, Iceland and a general study by the Energy Development Corporation, Philippines.

2.3.1 Soda Lake Geothermal Field

In 2009-2011 deflagration was carried out on three wells at Soda Lake Geothermal Field, Nevada, USA (Ohren et al., 2011). Combined stimulation operations on the first two wells did improve the well performance. However the individual efficacy of the deflagration cannot be determined due to the simultaneous operations, which were liner removal and casing perforation.

In a third well the deflagration is reported to increase the injection capacity by around 2 orders of magnitude (Ohren et al., 2011). However this does not account for the fact that this was achieved by a combination of deflagration and thermal stimulation by five days of cold water injection. The actual change in injection capacity before and after the deflagration alone was from 7gpm at a well head pressure (WHP) of 140psi and immediately after deflagration the capacity was around 30gpm at WHP of 150psi. This still represents a significant increase, although the numbers are not directly comparable due to the difference in the reported WHP. The remainder of the increase occurred as the result of long term injection, though whether the injection stimulation would have been effective without the prior deflagration is not known.

2.3.2 Reykjanes Geothermal Field

Following the promising results from Soda Lake, further deflagration trials were carried out at Reykjanes Geothermal Field in Iceland from 2010-2013. Four wells have been deflagrated in an initial trial (Sigurdsson, 2015). Well stimulation is commonly achieved in Iceland by thermal shocking, after which further stimulation may be required. Deflagration is an attractive option for further stimulation in Iceland as hydraulic fracturing has cost and availability issues, and acidising is ineffective in the basaltic lithology (Sigurdsson, 2015).

Injectivity index testing was inconclusive in two of the four wells due to unstable or limited well testing conditions. Close examination of the published results shows that in the best case the injectivity increased by 30% after eight shots at seven depths in the well. In another case the injectivity increase was negligible at 7% after five shots at four depths in the well. These percentages are based on short-term apparent injectivity readings (1.5 hour apparent injectivity) which are not as reliable as long-term testing. The conclusion from the Icelandic experience is that deflagration does increase permeability in the near-well region, though not as much as was hoped (Sigurdsson, 2015). It is acknowledged that this can be at least partially attributed to difficulty with accurately locating feed zones in the well, rather than inherent ineffectiveness of the deflagration process.

2.3.3 Energy Development Corporation

The Energy Development Corporation (EDC) of the Philippines is planning a deflagration trial program (Aspiras et al., 2015). A matrix has been developed for the evaluation of candidate wells for deflagration. Candidates are ranked on reservoir and well factors including the location of the well within the field, proximity and average capacity of nearby wells, shut-in temperature, permeability, skin factor and injectivity. In each well multiple target depths are ranked based on factors including lithology, rock compressive strength, fracture interconnectivity and fracture/fault orientation with respect to principal stress direction.

3. DEFLAGRATION OF BR66 AT OHAAKI

3.1 BR66 well details

The production well BR66 was drilled in 2013 to a depth of 2783 metres below casing head flange (mCHF) with an average deviation of approximately 13°. The 9-5/8" production casing is set at 1498 mCHF then a 7" perforated liner to total depth. The value for injectivity obtained at the completion test at a depth of 2120 mCHF was 9 t/h/bar, which is considered to be low for this area. This was measured in open hole prior to running the perforated liner. A subsequent flowing PTS survey confirmed the major feed zone to be around 2120 mCHF and the productivity index to be <1 t/h/bar. The well is very hot with a maximum measured temperature of 310°C. An acoustic televiewer (AFIT) log was run over the interval 2028-2489 mCHF, revealing high fracture density corresponding to the 2120 mCHF feed zone.

The well was selected for deflagration due to the combination of high temperature with low permeability, proximity to deep permeability feeding other producing wells and the high quality of data available, in particular the recent pressure-temperature-spinner (PTS) surveys and the AFIT log.

A review of the completion test data identifies the feed zones in the well to be at 1880, 2120 and 2270 mCHF considered to be major, major and minor in size respectively. The feed zones are located based on injection temperature profiles, fluid velocity profiles during injection, AFIT log, static heat-up profiles, and temperature and fluid velocity profiles during flow testing. The upper two feed zones are located in the Tahorakuri Formation, a major regional unit containing ignimbrite and other volcanics. The lower feed zone is located near the contact zone with the Waikora Formation, a sedimentary unit often found towards the base of the Tahorakuri Formation.

3.2 BR66 deflagration job details

All of the downhole components required for the BR66 deflagration trial were provided by Precise Propellant Stimulation LLC. These were the solid fuel units, carrier and detonator assembly. The downhole equipment was run on a standard wireline truck. The main components of this setup were the e-line, connector, casing collar locator (CCL) and firing panel. A CCL was run with the deflagration gun string to ensure that the charges were located to avoid the casing joints which are not perforated. The CCL can be particularly troublesome inside perforated liner so it is very important to have an accurate casing tally for reference.

For the trials conducted by Contact the TP-J-3000 fuel units selected were the largest available, 700×91mm diameter with energy content 33 MJ. Six of these charges were assembled into one carrier with two carriers being run together for each shot to give a total of 12 charges per shot. For a single deflagration shot the total energy was 392 MJ. The combined length of gun and CCL was a little over 10m.

The original plan was to conduct two shots at 2120 mCHF with a short injection test in between the shots and a long injection test before and after the whole job. Immediately following the pre-job injection test the first shot was armed and run down to the target zone at 2120 mCHF. The subsequent short injection test indicated the first shot gave only a modest increase in injectivity index and so the decision was made to move the second shot to the second major feed at 1880 mCHF. The second deflagration shot was detonated and the final injection test commenced as soon as the gun was laid out on the surface.

3.3 Injection test design

A full injection test nearly 24 hours long was completed both pre-deflagration and post-deflagration. The same test design was used in order to promote comparability of results. The test had three increasing injection rates (approximately 37, 77, and 113 t/h) followed by a fall-off to zero flow. The pressure fall-off period allowed was nearly 10 hours, followed by a heating profile as the tool was removed from the well.

A wireline PTS tool was used to gather the data. Towards the end of each injection rate a number of well profiles were completed in order to obtain a fluid velocity profile. One profile was completed in the middle of the pre-deflagration fall-off, though this was not repeated in the post-deflagration fall-off due to the unexpectedly longevity of the disruption to the pressure data.

The stable pressures at each injection rate and the pressure fall-off were measured at a depth of 2120 mCHF, which had previously been interpreted as a major feed zone, and confirmed early in the injection test. The actual flow into the well was metered and logged at all times, including during the initial quenching, during the injection testing and during the deflagration operation itself. As two shots were fired in this well, a very short injection test of three hours with no fall-off was performed between the two shots to provide a rough estimate of the incremental change in injectivity.

4. RESULTS AND DISCUSSION

4.1 Injectivity index

Injectivity has been evaluated at 1900 mCHF and 2120 mCHF, near both deflagration shot depths. Both depths have been evaluated as it is known that the injectivity can vary with depth for a variety of reasons. Most common is the change in fluid density due to changing temperature of the fluid column at different injection rates. In this scenario generally an injectivity value evaluated above the major feed zone will be an underestimate and below will be an overestimate. In a case such as BR66 where there are two major feed zones, both depths need to be evaluated. In the results presented here (Table 1 and Figure 1) the injectivities from the two major feed zones are the same within error.

Table 1: Injectivity index (II) values at 2120 mCHF and 1900 mCHF pre-deflagration, after one deflagration shot, and after two deflagration shots.

Depth [m]	Pre-deflag II [t/h/bar]	II after one-shot [t/h/bar]	Change from pre-deflag	II after two shots[t/h/bar]	Change from pre-deflag
1900	6.0	7.0	+17%	9.3	+55%
2120	5.9	6.8	+17%	9.3	+57%

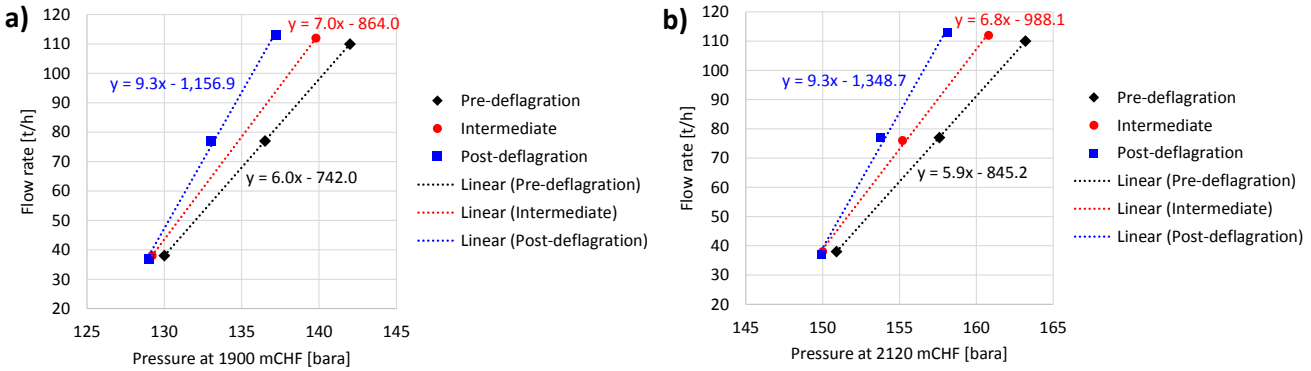

Figure 1: Injectivity index graphs for pre-deflagration, intermediate (after 1 shot) and post-deflagration (after 2 shots) testing: pressure data is taken from depths of a) 1900 mCHF; b) 2120 mCHF.

It can be seen from Figure 1 that each set of data points is quite linear and also that the lines nest together in a neat fan shape. For these two reasons it is considered that the values derived for injectivity index are reliable. This implies that despite the small scale of the increases in injectivity index of 17% and 57% (Table 1) they are likely to be real and not simply a fluctuation within error, or the result of unstable conditions during testing. It is unfortunately not possible to compare these values of injectivity to the value of 9 t/h/bar measured at the completion test in 2013 as the well conditions during testing were not the same as this was measured in open hole prior to running the liner.

4.2 Discussion of thermal permeability enhancement

As a large volume of cold water is injected into a hot reservoir, the injectivity of the well usually increases. Cessation of injection then results in a decrease in injectivity. The exact mechanism by which this reversible thermal effect occurs is not known. An empirical equation to describe the effect of temperature change on injectivity has been derived and published (Siega et al., 2014) based on a large volume of field data.

BR66 is a prime candidate for some thermal permeability enhancement due to the extreme temperature difference between the injectate and the very hot reservoir. Therefore the increase in injectivity after deflagration can be partially attributed to thermal permeability enhancement as a result of an extra 1.5 days of cold water injection prior to the post-deflagration test as compared to the pre-deflagration test. The equation derived by Siega et al. (2014) is used in order to obtain an estimate of the contribution of thermal permeability enhancement. The temperatures at the major feed zone during the post-deflagration test were 10°C lower on average than the pre-deflagration test. Using the empirical relationship the corresponding increase in injectivity index is predicted to be 11%. The overall change in injectivity after deflagration was around 57% (Table 1) which is much greater. It is therefore likely that the majority of the change in injectivity is the result of deflagration and not thermal permeability enhancement. A more conservative estimate of the change in injectivity would therefore be 46%.

4.3 Pressure transient analysis results

Pressure transient analysis (PTA) is undertaken in order to confirm the results for injectivity index. Also PTA can reveal whether the changes are a result of an increase in near-well permeability or wider reservoir permeability. Increase in near-well permeability (decrease in skin factor) is assumed to be the mechanism by which deflagration increases well performance. PTA is undertaken using both conventional analytical models using the software package SAPHIR™ and the TOUGH2 numerical models.

A pressure fall-off dataset of nearly ten hours duration is available from both the pre-deflagration and post-deflagration injection test. Only these pressure fall-off datasets have been subject to PTA because while the flow steps do yield a number of two-rate pressure transients, these are of a much shorter duration (2-3 hours). Also it was necessary to move the tool during these transients to obtain the profile data which resulted in large gaps in the pressure transient datasets.

Although special care was taken by the contractors to shut down the flow for the pressure fall-off as quickly as possible, it is never possible to achieve a perfect step-change. Very minor rounding of the pressure fall-off datasets was corrected using the cut-shift-fill

method (McLean and Zarrouk, 2015d). A derivative plot of both the pre-deflagration and post-deflagration fall-off is given in Figure 2 along with approximate indications of the durations of early-time, intermediate-time and late-time, which will be referred to throughout this study.

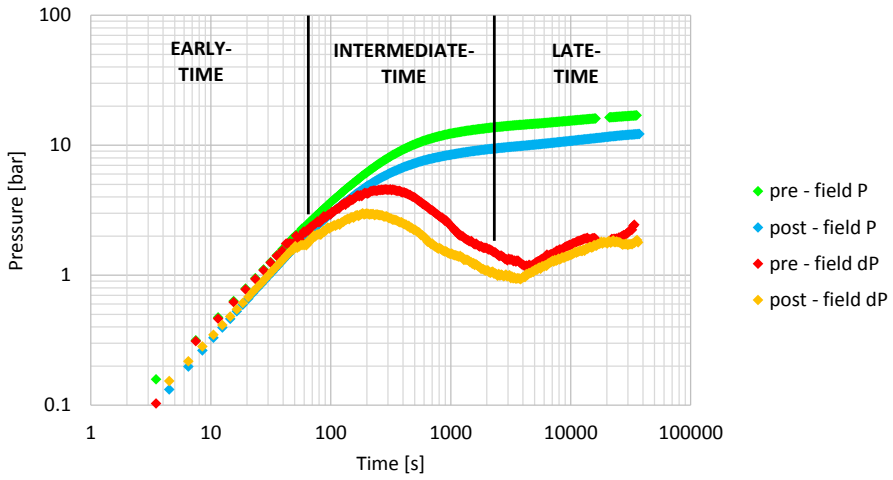

Figure 2: Log-log plot of pressure and pressure derivative for pre-deflagration (green and red) and post-deflagration (blue and yellow) fall-off datasets.

Various observations can be made from the shape of the pressure derivatives (Figure 2) in the context of published derivative shapes from analytical models (Horne, 1995). The derivatives have a unit slope and hump in early and intermediate-time, corresponding to a flow regime dominated by wellbore storage and skin. In late-time the derivatives begin to flatten off to a constant value as would be expected for an infinite-acting flow regime, but then increase before flattening again at a higher level. This dip, rise and subsequent flattening is reminiscent of both the published linear impermeable boundary response, and a dual-porosity reservoir response (Horne, 1995). At the end of the datasets both derivatives kick up slightly and without a longer test it is not clear whether this is a real response or an artifact of calculating a gradient near the end of a dataset.

For this study three different reservoir/boundary models are applied to the field data:

- Model 1: Infinite uniform porous reservoir (Figure 3)
- Model 2: Uniform porous reservoir with a linear impermeable boundary (Figure 4)
- Model 3: Infinite dual-porosity reservoir (Figure 5)

All three models are available for analytical analysis using SAPHIR^{TM}. Unfortunately a dual porosity model is not yet implemented for the numerical model setup, though this is the subject of current work using the multiple-interconnected (MINC) capability of TOUGH2. All analytical and numerical analyses have wellbore storage and skin. The infinite uniform porous reservoir model is included for interest and comparison, although it is not of an appropriate shape to match the data.

This is an inverse modelling process of fitting models to field data to estimate model parameters. For the analytical models the non-linear regression capability of SAPHIR^{TM} is used. For the numerical models both a manual process and non-linear regression have been used. The numerical non-linear regression is performed using PEST (Doherty, 2005) which will be described in more detail in Section 4.5.

The estimated parameters obtained for all model fits are summarised in Table 2. Log-log plots display the match between the models and field data in Figure 3, 4 and 5 for Models 1, 2 and 3 respectively. The main parameters of interest in Table 2 are the reservoir permeability k and the skin factor s. Also included are values for permeability in the skin zone calculated from the skin factor using Equation 1 and assuming a skin zone radius of 5m and using the known well radius of 0.1m:

$$s = \left(\frac{k_r}{k_s} - 1 \right) \ln \left(\frac{r_s}{r_w} \right) \quad (1)$$

where s, k_r, k_s, r_s, r_w are skin factor, reservoir permeability, skin zone permeability, skin zone radius and well radius, respectively.

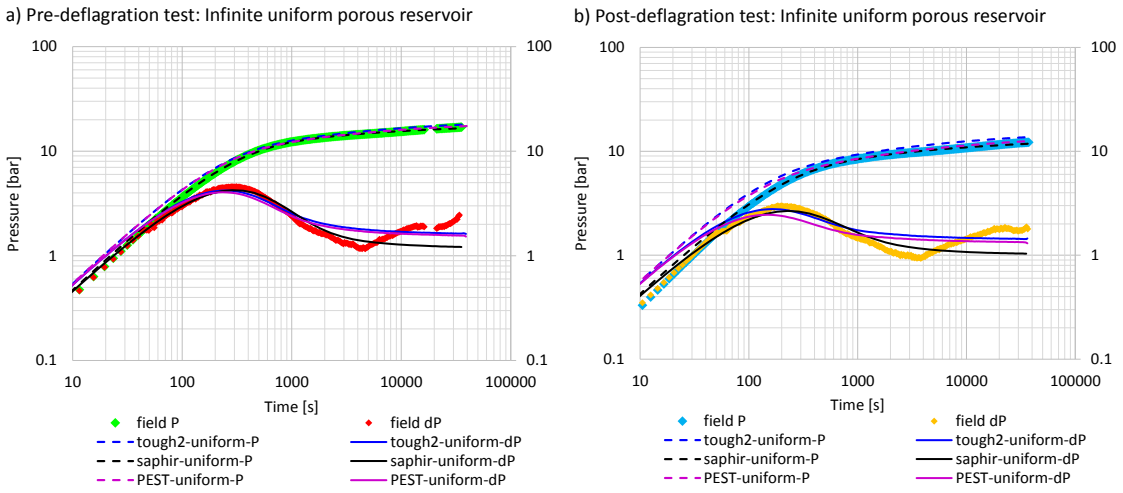

Figure 3: Log-log plots of pressure and pressure derivative for Model 1 (infinite uniform porous reservoir): analytical non-linear regression (black), numerical manual fit (blue) and numerical non-linear regression (purple): a) pre-deflagration; b) post-deflagration.

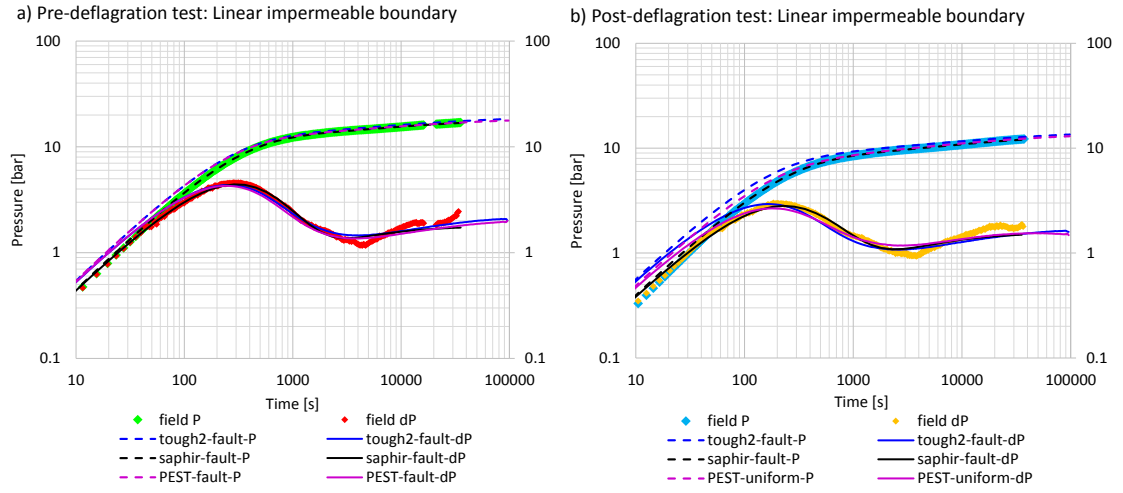

Figure 4: Log-log plots of pressure and pressure derivative for Model 2 (linear impermeable boundary): analytical non-linear regression (black), numerical manual fit (blue) and numerical non-linear regression (purple): a) pre-deflagration; b) post-deflagration.

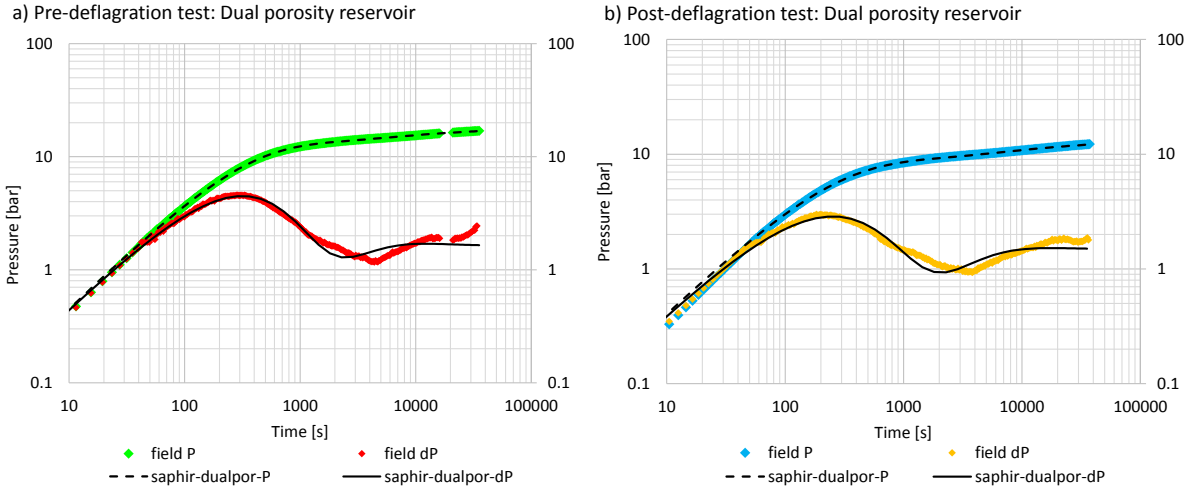

Figure 5: Log-log plots of pressure and pressure derivative for Model 3 (dual porosity): analytical non-linear regression (black): a) pre-deflagration; b) post-deflagration.

Table 2: Model parameters estimated by inverse modelling using field datasets

Model	Parameter *	Analytical (SAPHIR™) results			Numerical (TOUGH2) results – manual fit			Numerical (TOUGH2) results – PEST fit		
		Pre-deflag	Post-deflag	Change	Pre-deflag	Post-deflag	Change	Pre-deflag	Post-deflag	Change
Infinite uniform porous	k [mD]	2.9 (2.8-2.9)**	3.4 (3.4 to 3.5)	+20%	3	3.5	+17%	3.1 (3.1 to 3.2)	3.8 (3.7 to 3.8)	+20%
	s	0.8 (0.6-0.9)	-0.5 (-0.6 to -0.4)	-1.3	-2.8	-3.3	-0.5	-2.8 (-2.8 to -2.8)	-3.3 (-3.4 to -3.3)	-0.5
	calculated ks [mD]	2.4	4.0	+67%	10.6	22.4	+111%	10.9	25.6	+135%
Linear imperm. boundary	k [mD]	3.8 (3.7-3.8)	4.5 (4.3 to 4.7)	+18%	4	5.5	+38%	4.3 (4.3 to 4.4)	4.8 (4.8 to 4.8)	+11%
	s	2.4 (2.4-2.5)	0.7 (0.4 to 0.9)	-1.8	-2.5	-3	-0.5	-2.4 (-2.4 to -2.4)	-3.1 (-3.1 to -3.0)	-0.7
	calculated ks [mD]	2.3	3.8	+63%	11.1	23.6	+113%	11.1	21.9	+97%
	L [m]	19.9 (19.5-20.4)	22.5 (20.7 to 24.5)	negli-gible	30	30	none	30 (fixed)	30 (fixed)	n/a
Dual porosity	k [mD]	2.1 (2.1-2.2)	2.4 (2.3 to 2.4)	+12%						
	s	-0.8 (-0.9 to -0.7)	-2.0 (-2.2 to -2.0)	-1.2						
	calculated ks [mD]	2.7	5.0	+86%						

* k [mD] = reservoir permeability; s = skin factor [dimensionless]; ks [mD] = skin zone permeability
** all ranges in brackets represent 95% confidence intervals from non-linear regression, to one decimal place.

4.4 Observations from comparison of numerical and analytical PTA results

Skin factors are significantly higher for the analytical models compared to the numerical models, to the extent they are often positive (Table 2). All the numerical skin factors are significantly negative. This discrepancy is attributed to the fact that analytical models do not take account of the injectate temperature effect, which looks like positive skin (McLean and Zarrouk, 2015b). Numerical models are able to account for this effect and for this reason the results from numerical modelling are considered to be more representative. The negative skin factors obtained by numerical modelling are also more plausible as BR66 was drilled with water and air to remove cuttings, and no drilling mud, so there is no reason to anticipate positive skin.

The following observations have been made from comparison of the Model 1 (infinite uniform porous reservoir) results:

- For the numerical inversions the manual and non-linear regression results are the same within error. These are an increase in reservoir permeability of 17% and 20% respectively, and an increase in skin zone permeability of approximately 111% and 135%. The skin factors are significantly negative (a change from -2.8 to -3.3 for both models).
- The analytical result for reservoir permeability is the same with an overall increase of 20%. The actual values are very similar as well with 2.9 mD (analytical) compared to 3.0 or 3.1 mD (numerical) for pre-deflagration. Post-deflagration values are 3.4 mD (analytical) compared to 3.5 or 3.8 mD (numerical).
- The analytical results for skin are quite different, with a smaller increase in skin zone permeability of approximately 67%, approximately half the numerical value. The skin factor goes from positive to negative (0.8 to -0.5). A real positive skin factor is highly unlikely in this well as previously discussed and these results are not considered to be reliable.
- The fit of these three infinite uniform porous reservoir models to the field data is poor, both numerical and analytical, as they cut through the shape of the derivative in late-time (Figure 3).
- The analytical model derivatives are a slightly different shape to the numerical equivalents, passing lower through the field data in late-time (Figure 3). This may be due to some weighting of the objective function or other detail of the non-linear regression process built into SAPHIR™.

The following observations have been made from comparison of Model 2 (linear impermeable boundary) results:

- For the numerical inversions the manual and non-linear regression results are similar, though not as close as for Model 1. This may be simply the result of using a slightly more complex model with an extra parameter. The numerical manual and non-linear regression results are an overall increase in reservoir permeability of 38% and 11% respectively.
- The numerical model overall increases in skin zone permeability is very similar with 113% and 97% for manual and non-linear regression respectively. The actual values for skin factor are also very similar, and significantly negative, with pre-deflagration values of -2.5 compared to -2.4 and post-deflagration values of -3.0 compared to -3.1.
- The analytical model values for reservoir permeability are slightly lower than the numerical values, however the overall change is similar with a value of 18%.
- The analytical skin factor is significantly different with positive values of 2.4 pre-deflagration and 0.7 post-deflagration. The overall change in skin zone permeability is 63%, around half of the numerical equivalent value, a similar observation to the Model 1 results. Analytically derived skin factors are not considered to be reliable.
- The fit of these three linear impermeable boundary models to the field data is reasonable, producing a close approximation of the derivative shape of the field data (Figure 4).
- All three linear impermeable boundary model derivative shapes are extremely similar (Figure 4) regardless of manual inversion or non-linear regression, whether numerical or analytical.

As no numerical dual porosity model is yet available, not much discussion of these analytical results is possible. The fit of the analytical dual porosity model to the field data is also reasonable, producing a close approximation of the derivative shape (Figure 5).

For all models there is a significant increase in permeability of the skin zone (decrease in skin factor), which is an expected result of the deflagration. For all models there is also a minor increase in the permeability of the wider reservoir, which is not expected as the mechanism of deflagration affects only the near-wellbore region. This increase could indicate that the effect of deflagration extended further into the reservoir than anticipated, producing an apparent increase without truly affecting the permeability a significant distance from the well. It is possible that if the width of the skin zone in the model was increased, this apparent increase in reservoir permeability would disappear. These increases in permeability are consistent with the increase in injectivity index of the well.

4.5 Non-linear regression with model-independent parameter estimation (PEST)

The initial numerical inverse modelling was completed manually, followed by non-linear regression for comparison. Although the manual process is not a mathematically rigorous one it does produce a good match within a reasonable timeframe as the model is simple and runs quickly. It also allows the reservoir engineer to develop a good understanding of the sensitivity of the pressure derivative plot results to the various model parameters. Non-linear regression has been performed using the capability of PEST (Doherty, 2005). Both the field data and the model output are interpolated onto a set of log-spaced times, with 100 points per log cycle. This prevents the result from being biased by the relatively large number of data points available in late-time as compared to early-time. The interpolation also produces two datasets with data points at exactly the same times, which is necessary for direct comparison. The subsequent non-linear regression is a simple one with no weighting of the objective function.

Non-linear regression with the infinite uniform porous reservoir model was straightforward with two variable parameters (reservoir permeability and skin) and produced the same match regardless of the starting point in parameter space. The results were extremely similar to the results of the manual process (Figure 3, Table 2). Non-linear regression of the linear impermeable boundary model was not straightforward and a number of different inversions were run in order to investigate, with different starting points in parameter space for the three parameters (reservoir permeability, skin and boundary distance). For most inversions, the result was for a boundary at 67m (Figure 6), which seems to be the true minimum of the least squares objective function with a value of phi = 15. However it can be seen in Figure 6 that this derivative cuts through the intermediate and late-time field data without reproducing the significant dip and rise of the field data. Only one inversion gave a reasonable derivative shape, with the boundary at 20m. However this was only achieved by setting the initial value to 20m and the value barely changed during the iterations. This match must represent a local minimum in the objective function, and has a value of phi = 27. As a temporary measure in order to overcome these difficulties, some bias was added into the process by fixing the boundary distance to be 30m (results in Table 2), which is known from the manual results to best represent the shape of the derivative (Figure 4, Table 2). Instead of fixing parameters it is possible that the fit from the PEST non-linear regression could be improved by weighting the objective function (phi), and this will be the subject of further work. Other work will build the non-linear regression capability directly into the PyTOUGH script, to promote user-friendliness.

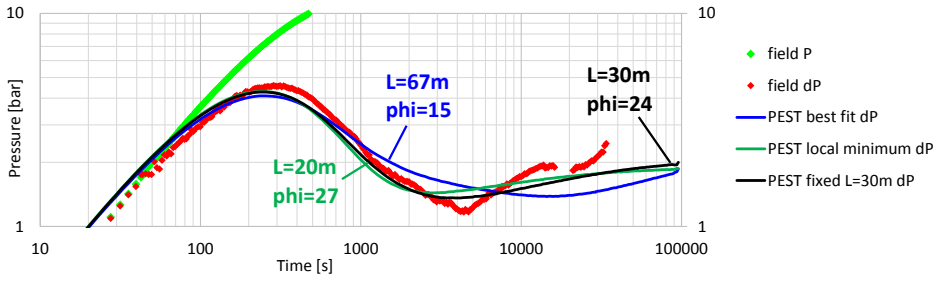

Figure 6: PEST non-linear regression results: variation of pressure derivative with different input parameters.

Examination of the correlation coefficients reveals there is always an extremely high correlation between reservoir permeability and skin factor (97-99%). This is the case for both the PEST and SAPHIR^{TM} inversions. Therefore the 95% confidence intervals reported in Table 2 should be treated with caution. The high correlation is surprising as it was apparent during the manual process that the skin factor has more effect on the early or intermediate-time data and the reservoir permeability has more effect on the late-time data, and this will be the subject of further study.

4.6 Effect of changing injectate temperature in numerical model

Analytical models allow the specification of one fluid temperature only, and the reservoir temperature is usually used. The numerical models also require the specification of the temperature of the injection fluid, a significant advance (McLean and Zarrouk, 2015a). For this study the value used for injectate temperature is the temperature at the tool depth at the start of the pressure transient as recommended by McLean and Zarrouk (2015b). These values were 57°C and 43°C for the pre-deflagration and post-deflagration analyses, both measured at the tool depth of 2120 mCHF. This recommendation is based on practicality, however an average temperature across the reservoir interval can also be used, provided there is sufficient data available (McLean and Zarrouk, 2015b), which is the case for this study. Temperature values as an average from the uppermost feed zone to the maximum PTS profile depth (approx. 1900-2400 mCHF) are 88°C and 73°C for the pre-deflagration and post-deflagration test respectively. These were calculated from the temperature profile closest in time to the fall-off transient, during the third injection rate. Preference was given to profiles measured while the tool was moving down, as experience has shown that temperature is overestimated while a tool is moving up, most likely due to residual heat in the tool while moving away from deeper hotter fluids. The numerical manual analysis is re-done for Model 1 (infinite uniform porous reservoir) with the new values for injectate temperature, and the results compared in Table 3 to the original results from Table 2.

Table 3: Comparison of estimated model parameters for two methods of evaluating injectate temperature

Parameter	Method 1: one value at tool depth (results from Table 2)			Method 2: average over reservoir interval		
	Pre-deflag	Post-deflag	Change	Pre-deflag	Post-deflag	Change
Injectate temperature [°C]	57	43	n/a	88	73	n/a
Reservoir permeability: k [mD]	3	3.5	+17%	3	3.5	+17%
Skin factor: s	-2.8	-3.3	-0.5	-2.3	-3.0	-0.7
Skin zone permeability: ks [mD]	10.6	22.4	+111%	7.3	15.0	+105%

The values for reservoir permeability are exactly the same regardless of the injectate temperature, which is expected as the injectate temperature is known to affect the results for skin but not reservoir permeability (McLean and Zarrouk, 2015b). The values for skin factor are less, -2.3 and -3.0 for pre-deflagration and post-deflagration respectively, than the original results of -2.8 and -3.3. This is expected as injecting cold water produces a derivative hump shape which resembles positive skin. The higher the injectate temperature, the less of a derivative hump can be attributed to this temperature effect, and so more of the hump is attributed to positive skin (or less-negative skin in this case). The change in skin factor appears at first glance to be greater with a decrease of 0.7 as compared to 0.5 from the original results. However the actual change in skin zone permeability this represents is virtually the same within error with an increase of 105% as compared to the original 111%. It does seem reasonable to use the average temperature across the reservoir interval if that data is available, and the single transient depth value if it is not. Provided that the method of choice is consistent across all the numerical analyses, the overall outcome will not be affected.

4.7 Effect of changing layer thickness in numerical model

The standard model setup has been shown to yield results which are sensitive to the layer thickness of the model (McLean and Zarrouk, 2015a). It is recommended that the entire open-hole vertical thickness is used unless there is information to justify a lesser value. For the numerical model setup in this study the layer thickness is 600m, approximately half of the vertical thickness of the entire open-hole interval. This is considered to be justified as there is a large volume of high quality data for this well. The thickness has been refined to the vertical distance between the uppermost feed zone and the depth of the basement which is usually impermeable and shows no signs of permeability during any of the testing. The numerical manual analysis has been re-done for Model 2 (linear impermeable boundary) for a layer thickness of 1200m, representing the entire open-hole, and the results presented in Table 4.

Table 4: Comparison of estimated model parameters for two layer thicknesses in the numerical model

Parameter	Thickness = 600m (results from Table 2)			Thickness = 1200m		
	Pre-deflag	Post-deflag	Change	Pre-deflag	Post-deflag	Change
Reservoir permeability: k [mD]	4	5.5	+38%	1.9	2.7	+42%
Skin factor: s	-2.5	-3	-0.5	-2.2	-2.7	-0.5
Skin zone permeability: ks [mD]	11.1	23.6	+113%	4.3	8.7	+102%
Boundary-to-well distance: L [m]	30	30	none	25	25	none

The reservoir permeability is halved by a doubling of layer thickness, which is expected. Despite this, the overall change for each scenario is the same within error (38% compared to 42%). The actual values for skin factor are slightly increased by the doubling of the layer thickness but again the overall change is the same, a decrease of 0.5 for both scenarios. Also the overall change in calculated skin factor is the same within error (113% compared to 102%). The boundary distance is not particularly well constrained and so a change from 30m to 25m is considered insignificant. As a result of changing the layer thickness, no significant difference is observed in the overall pre-deflagration and post-deflagration change for any of the parameters.

5. CONCLUSIONS

The overall change in injectivity index as a result of deflagration is 57% (5.9 to 9.3 t/h/bar). The contribution of thermal permeability enhancement to this change is estimated to be 11%. A conservative estimate of the change in injectivity index as a result of deflagration alone is therefore 46%.

The results of PTA indicate an increase in both near-wellbore and wider reservoir permeability, which is consistent with the measured increase in injectivity. The near-wellbore permeability approximately doubles, while the reservoir permeability has a more modest increase of approximately 20%. There is no mechanism to produce an increase in the permeability of the wider reservoir, and so this apparent increase is attributed to the extension of the stimulation slightly beyond the modelled skin zone.

The numerical standard model setup is demonstrated to be effective at producing meaningful results for geothermal PTA. The choice of method used to assess the injectate temperature does not affect the overall results in percentage terms, though it will affect the exact value of the skin factor. The choice of layer thickness will also not affect the overall results, but will affect the exact value of the reservoir permeability and skin factor. These sensitivities are not an issue provided there is consistency in method when setting up the models.

Deflagration produces a small but measureable increase in well performance, consistent with the Icelandic experience.

ACKNOWLEDGEMENTS

Contact Energy is acknowledged for access to field data and the ongoing support.

REFERENCES

Aspiras, A.H., Braganza, J.S., Morente, C.P., Austria, J.J.C., Jumawan, J.E., and Whittome, A.J.: Selection of Candidate Geothermal Wells for Deflagration, *Proceedings*, 37th New Zealand Geothermal Workshop, Taupo, New Zealand (2015).

Croucher, A.E.: PyTOUGH: a Python Scripting Library for Automating TOUGH2 simulations, *Proceedings*, 33rd New Zealand Geothermal Workshop, Auckland, New Zealand (2011).

Doherty, J.: PEST Model-Independent Parameter Estimation User Manual, Watermark Numerical Computing (2005).

Horne, R.N.: Modern Well Test Analysis: A Computer-Aided Approach, *2nd Ed.*, Petroway Inc (1995).

McLean, K., and Zarrouk, S.J.: Standardised Reservoir Model Design for Simulating Pressure Transients in Geothermal Wells, *Proceedings*, 37th New Zealand Geothermal Workshop, Taupo, New Zealand (2015a).

McLean, K., and Zarrouk, S.J.: Impact of Cold Water Injection on Geothermal Pressure Transient Analysis: A Reservoir Modelling Assessment, *Proceedings*, 37th New Zealand Geothermal Workshop, Taupo, New Zealand (2015b).

McLean, K., and Zarrouk, S.J.: Linear Impermeable Boundary in Geothermal Pressure Transient Analysis: A Reservoir Modelling Assessment, *Proceedings*, 37th New Zealand Geothermal Workshop, Taupo, New Zealand (2015c).

McLean, K., and Zarrouk, S.J.: Geothermal Well Test Analysis Using the Pressure Derivative: Some Common Issues and Solutions, *Geothermics*, **55**, (2015d), 108-125.

Ohren, M., Benoit, D., Kumataka, M., and Morrison, M.: Permeability Recovery and Enhancements in the Soda Lake Geothermal Field, Fallon, Nevada, *Geothermal Resource Council Transactions*, **35**, (2011), 493-497.

Pruess, K.: TOUGH2: A general-purpose numerical simulator for multiphase fluid and heat flow, *Lawrence Berkeley Report No. LBL-29400*, Berkeley, California (1991).

Siega, C., Grant, M.A., Bixley, P.F., and Mannington, W.: Quantifying the Effect of Temperature on Well Injectivity, *Proceedings*, 36th New Zealand Geothermal Workshop, Auckland, New Zealand (2014).

Sigurdsson, O.: Experimenting with Deflagration for Stimulating Geothermal Wells, *Proceedings*, World Geothermal Congress, Melbourne, Australia (2015).

Yeh, A., Croucher, A. and O'Sullivan, M.J.: Recent developments in the AUTOUGH2 simulator, *Proceedings*, TOUGH Symposium 2012, Berkeley, California, September 17-19 (2012).